Near Surface Geophysics, 2014, **12**, 35-43 doi:10.3997/1873-0604.2013035

Soil resistivity monitoring of an irrigation experiment

Torleif Dahlin[1*], Pär Aronsson[2] and Mats Thörnelöf[3]

[1] *Engineering Geology, Lund University, Box 118, SE-221 00 Lund, Sweden*
[2] *Swedish University of Agricultural Sciences, Department of Crop Production Ecology, P.O. Box 7043, SE-750 07 Uppsala, Sweden*
[3] *Swedish Geological Survey, Box 670, SE-751 28 Uppsala, Sweden*

Received May 2012, revision accepted March 2013

ABSTRACT

Resistivity measurements were used for tracing water transport during a three-year irrigation study. Three different rates of landfill leachate irrigation and one control treatment were applied to two cultivars of short-rotation willow coppice. Groundwater level measurements and water sampling were carried out in pipes installed in the centre of each plot. Resistivity was measured with permanently installed electrodes along six lines running through the centre of the plots. The resistivity results were inverted to produce vertical sections of ground resistivity at different time steps and as change in resistivity relative to the start of the experiment. Changes in resistivity linked to differences in irrigation quantities and plant growth were observed. The results showed that a repeated soil resistivity measurement has the potential as a tool to monitor changes in soil water and ion contents. Furthermore, expanding zones of increasing soil resistivity immediately under and around the plants indicate that the method may be useful for imaging plant root development.

INTRODUCTION

Mixed landfills with household waste as a major component generate leachate as a result of infiltrating precipitation and degradation of organic waste within the landfill. This leachate usually contains high concentrations of nitrogen and salts (e.g., Öman *et al*. 2000). Swedish landfill leachate typically contains some 200–400 mg/L of nitrogen (mainly ammonium) and sodium chloride in concentrations typically in the range of 800–1800 mg/L. In Sweden, landfill leachate is treated on some locations with different types of 'ecological' treatment methods, including the use of constructed wetlands and use of leachate in the irrigation of crops. The driving force behind this is partly economic considerations and partly a search for more efficient treatment methods, as the chemical composition of landfill leachate makes it difficult to treat.

Short-rotation willow coppice (SRWC) produced for energy purposes is a fully mechanised commercial cropping system in Sweden. The crop is relatively cheap to establish, grows rapidly and is harvested every 3–5 years. These properties together with the fact that it is a non-food and non-fodder crop make it an interesting crop for 'ecological engineering' purposes. During the 1990s, several systems were established in Sweden for treating landfill leachate by irrigation of SRWC established either on restored parts of landfills or on adjacent arable fields (Dimitriou and Aronsson 2007).

Resistivity mapping with limited depth resolution but good area cover is an emerging tool for mapping variations in physico-chemical soil parameters for precision agriculture (e.g., Gebbers *et al*. 2009; Besson *et al*. 2010). Soil resistivity measurements have also been identified as potentially useful for mapping soil compaction (Seladj *et al*. 2010). Two-dimensional (2D) resistivity imaging based on surface measurements, also known as electrical resistance tomography (ERT) or continuous vertical electrical sounding (CVES), is now a standard procedure for environmental and engineering applications (e.g., Dahlin 2001; Auken *et al*. 2006). Such analyses result in inverted model sections showing the variation in resistivity in cross-sections of the ground. Based on an experiment in an orchard, Rossi *et al*. (2011) concluded that resistivity imaging is a promising tool for estimating root biomass density. A time series of resistivity imaging has been successfully applied for imaging the spatial and seasonal variations in water and ion content in saturated and unsaturated zones (e.g., Hagrey *et al*. 1999; Slater and Sandberg 2000; Kemna *et al*. 2002; French and Binley 2004; Leroux and Dahlin 2005). The results have been validated by laboratory experiments (Binley *et al*. 1996). Jones *et al*. (2009) used electrical resistivity imaging for monitoring subsidence arising from when tree roots absorb water from clay-rich soils and demonstrated its capability to outline distribution and variation in activity of the tree root system. Samouëlian *et al*. (2004) used resistivity monitoring to follow the development of soil cracks when a soil block dried. In landfill applications, time-lapse resistivity studies have shown good potential for tracing water flow in connection with leachate recirculation tests (e.g., Guerin *et al*. 2004; Rosqvist *et al*. 2005). In another example of time-lapse monitoring, Sjödahl *et al*. (2008) used resistivity monitoring for detecting anomalous seepage through an earth embankment dam.

* torleif.dahlin@tg.lth.se

© 2014 European Association of Geoscientists & Engineers

In this paper we report results from a three-year field study of irrigation of SRWC with landfill leachate. The part of the study reported upon here comprised eight plots supplied with landfill leachate from a commercial landfill and the aim was to use soil resistivity measurements for tracing leachate transport in the soil. Results from the same field trial concerning the effects on plants and treatment efficiency in terms of retention of plant nutrients and heavy metals are presented in a previous paper (Aronsson *et al*. 2010).

OBJECTIVES

The specific objectives of the study were to:

- Assess the change in soil resistivity in SRWC irrigated with landfill leachate, as a tool to image the zone affected by irrigation
- Image the lateral transport of water in the saturated zone and assess the usefulness of groundwater sampling methodology.

An unplanned outcome was that zones of increasing resistivity indicated that soil resistivity measurements might be used to follow the development of plant root systems over time and this was therefore included when analysing and interpreting the data.

MATERIALS AND METHODS

Site and plants

The field trial was established on an arable field adjacent to a large, commercial landfill operated by Ragn-Sells Avfallsbehandling AB, Upplands-Bro, Sweden (59°33'08 N; 17°37'25 E). The trial originally comprised sixteen 400 m^2 square plots divided into two blocks according to an assumed gradient in the groundwater level, controlling the direction of flow of the groundwater. For the study reported here, only the NW block was used (i.e., eight plots). Four treatments were applied (see below) with two replicates each for the two willow cultivars tested. The soil at the site is a heavy clay soil with 34–42% clay content and a humus content of 14–25% in the topsoil. During 18–19 May 2005, cuttings of two commercial cultivars of willow, cv. Tora and cv. Gudrun, were planted manually in a double-row system with 1.5 m between the double rows, 0.75 m between the rows within the double row and a spacing of 0.6 m between plants in the rows. This corresponds to the way commercial willow plantations are established in Sweden. After planting, a sprinkler irrigation system was established in order to prevent drought damage before the onset of leachate irrigation. Pressure regulated drip irrigation pipes were laid out in every double row in order to ensure a very even distribution of the landfill leachate.

Treatments

Three different rates of landfill leachate irrigation and one control treatment were applied in a split-plot design with the irrigation rate on one axis and the cultivar on the other (Fig. 1). A system was installed to allow soil resistivity measurements along six lines (see further description below). In the centre of each plot, two groundwater pipes were installed, at 0.8 and 1.3 m depth respectively, for measurement of the groundwater level and for sampling of superficial groundwater (for further description see Aronsson *et al*. 2010). The photographs in Fig. 2 show the site at two stages during the first year.

The irrigation water used in the trial was pre-treated in a nitrification/denitrification facility. The three levels of leachate irrigation corresponded to 1 (Trtm 1), 2 (Trtm 2) and 3 (Trtm 3) times the pre-calculated average precipitation deficit, i.e., the difference between normal precipitation and estimated evapotranspiration during the summer period. The control (Ctrl) treatment was not irrigated during the first growing season (i.e., 2005) but during 2006 and 2007 it was irrigated with tap water in the same amounts as treatment 1. The start and end of irrigation in each season, accumulated irrigation load and concentration of chloride (Cl^-) and average electric conductivity in the landfill leachate used for irrigation are presented in Table 1. The loads of chloride as a result of leachate irrigation were 2870, 5740 and 8600 kg Cl^-/ha during 2007 for treatments 1, 2 and 3, respectively (data not shown).

Plant growth estimation

The annual growth of the willow plants was estimated using a combination of destructive and non-destructive measurements in a central 10 m x 10 m net plot of each experimental plot. The shoot diameter at 1.0 m height of all living shoots of 10 sampling plants in each net plot was measured. For each willow cultivar, a set of 25 shoots was then harvested in order to determine the allometric relationship between the shoot diameter and shoot dry weight according to:

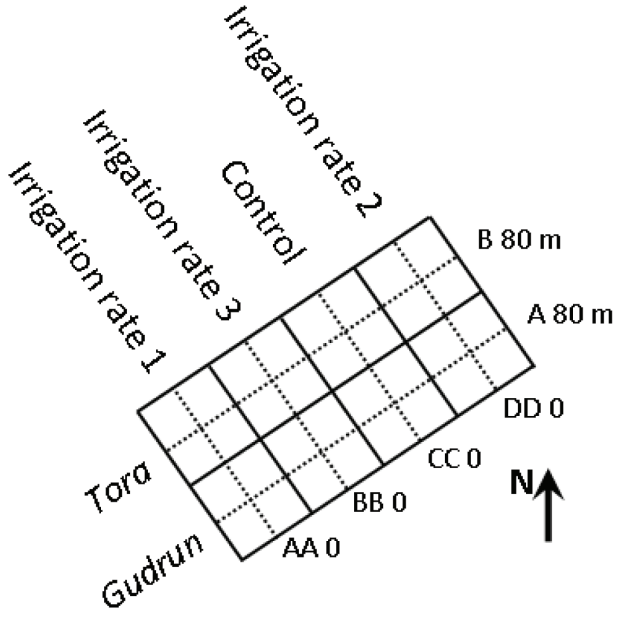


FIGURE 1
Design of the field trial with a willow cultivar. Treatment and lines for soil resistivity measurements indicated by lines.

$$Shoot\ dry\ weight = a * diameter^{b} \quad (1)$$

where a and b are parameters obtained through non-linear regression using SIGMA Plot software. The shoot dry weight of each sampled plant was calculated using equation (1). For each net plot, the mean plant weight was calculated and multiplied by the number of living plants in the net plot in order to achieve an estimate of the total plant dry weight of each plot.

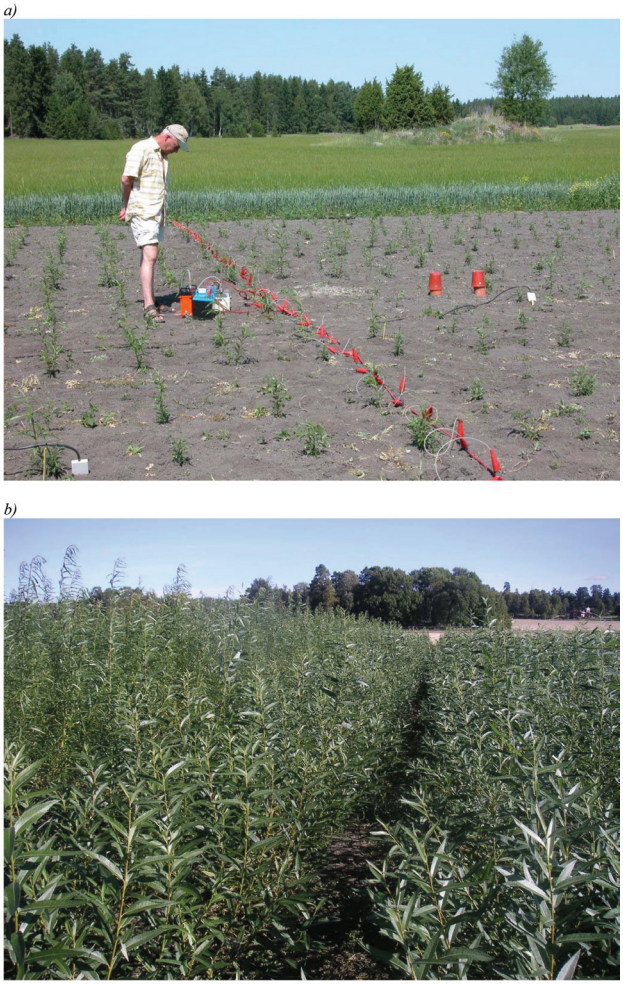


FIGURE 2
Photographs showing the field site; a) at an early stage of the experiment (6 July 2005), b) at the end of the first growing season (19 September 2005).

Groundwater sampling

To install the groundwater pipes, two holes were drilled, to a depth of 0.8 and 1.3 m respectively, using an auger. PVC pipes with a diameter of 50 mm and slotted from the bottom up to 0.5 m from the soil surface were installed into the holes according to a procedure described by Aronsson *et al*. (2010). In each pipe, a 10 mm PET suction pipe was installed for sampling of the groundwater by a vacuum pump. The groundwater level was recorded weekly during the irrigation season using a plumb bob. Samples for chemical analyses were taken biweekly during the irrigation season and at longer intervals during other periods of the year. The sampling method required the most superficial groundwater to be sampled and therefore sampling was always carried out in the 0.8 m deep pipe if possible, in order to retrieve water samples that best reflected the percolating water leaving the root zone.

Any lateral transport of groundwater between the plots would have reduced the usefulness of the samples for leaching estimates. Assessing such a lateral flow was therefore one of the main objectives of the study. When presenting data on concentrations and water balance, mean values of the two observations per treatment are used, i.e., groundwater data for the two willow cultivars were pooled.

Resistivity imaging

Repeated resistivity measurements were carried out along six lines referred to as A, B, AA, BB, CC and DD, as shown in Fig. 1. The resistivity surveying was carried out as 2D resistivity imaging. A photograph from an early stage of the field measurements is shown in Fig. 2(a).

The resistivity method measures variations in the electrical resistivity of the ground by applying electrical currents across arrays of electrodes inserted into the ground. During resistivity surveys, a current is injected into the ground through a pair of current electrodes and the potential difference is measured simultaneously between one or several pairs of potential electrodes. The current and potential electrodes are generally arranged in a linear array. In most common soil and rock types, the electrical charge is transported by electrolytic conductivity (e.g., Palacky 1987).

The resistivity data were collected using the ABEM Lund Imaging System, a computer controlled multi-electrode data acquisition system used for 2D and 3D high-resolution surveys

TABLE 1
Data on irrigation practices, accumulated irrigation loads, mean concentration of chloride and mean electrical conductivity in the irrigation water applied in the control and treatments 1–3.

			Irrigation load (mm)					
Year	**Start irrig.**	**End irrig.**	**Ctrl**	**Trtm 1**	**Trtm 2**	**Trtm 3**	**Chloride conc. (mg/L)**	**Conductivity (mS/m)**
2005	20 Jul	27 Sept	33	33	66	99	1090	769
2006	01 Jun	21 Sep	164	164	238	492	1320	694
2007	11 May	28 Sep	282	282	564	846	1020	554

consisting in a resistivity meter, a relay switching unit, multi-electrode cables and stainless steel electrodes (Dahlin 2001). In this case, four multi-electrode cables with 21 take-outs each were used, giving a total of 81 active electrodes per line due to overlapping take-outs at cable ends. A multiple gradient array was used for the measurements (Dahlin and Zhou 2006). The spacing between the electrodes was 1 m (lines A and B) or 0.5 m (lines AA, BB, CC and DD). Resistivity measurements were made on 20 occasions during the study.

The stainless steel electrodes used were left in the ground throughout the experiment in order to avoid positioning errors and the electrode cable was hooked up to these during each field measurement session. Staff at the waste management company, with no previous experience of geophysics, were instructed during the initial round of sampling and carried out the field data acquisition with minimal support thereafter.

The resistivity readings were processed to produce sections of the subsurface resistivity distribution. Inverse numerical modelling (inversion) was used to produce model sections of the estimated distribution of resistivity in cross-sections through the ground using an approach described by Loke *et al*. (2003). The change in resistivity relative to the first measurement occasion was assessed using time-lapse inversion (e.g., Sjödahl *et al*. 2008) and the result was plotted as relative change in resistivity. The inversion was performed using Res2dinv (version 3.55.73) and a robust (L1-norm) constraint was used in space and time.

The results were combined with available information on the soil, groundwater level and groundwater chemistry in order to provide information on the subsurface structure and the water and ion distribution, including the change in these over time.

RESULTS

Growth

During the first growing season, i.e., 2005, willow growth corresponded to 0.8–1.8 tonnes of dry matter (DM) per hectare (Fig. 3). During 2006, plant growth was very high in general but also highly variable (i.e., 2.4–13.7 tonnes DM/ha). It was higher in cv. Gudrun (10.2 tonnes DM/ha) than in cv. Tora (6.7 tonnes DM/ha). The lower growth in cv. Tora was mainly due to very poor growth in the plot with treatment 1 in the NW corner of the experimental field. During 2007, growth was even higher than in the previous year, 11.4 and 10.7 tonnes DM/ha for cvs. Gudrun and Tora, respectively. The growth in cv. Tora in treatment 1 seemed to have recovered considerably compared with 2006. The highest growth (16.9 tonnes DM/ha) was recorded for cv. Tora in the control treatment.

Groundwater level

The groundwater level varied considerably during the trial period, with clear peaks following intensive rain and snowmelt (Fig. 4). During the growing season, the depth to the groundwater varied between treatments.

Groundwater chloride concentration and electrical conductivity

The electrical conductivity and Cl^- concentration of the sampled superficial groundwater showed high variability between treatments and over time (Fig. 4). Irrigation with landfill leachate resulted in leaching of Cl^- to groundwater and elevated electrical conductivity of the groundwater. There was a tendency for plots with the highest load of leachate to also have the highest Cl^- concentrations in the groundwater. In the control treatment, electrical conductivity was low and with small variability over time. However there was a small increase in Cl^- concentration in the groundwater samples from the control treatment over time (Fig. 5).

Resistivity imaging

Initially, the measured lines showed largely similar resistivity structures in the investigated area, with resistivities of a few tens of Ωm in the upper parts of the soil profile (Fig. 6). This low resistivity reflects the high-clay content of the soil. The soil profile was divided into a 1–2 m upper layer with resistivity around 20–30 Ωm, underlain by a layer with lower resistivity. The lower part of the top layer coincided roughly with the groundwater level. The lower layer had resistivity around 10–15 Ωm along line A, whereas in the south-eastern part of the area (i.e., lower right-hand side in Fig. 6) it lay around 15–20 Ωm.

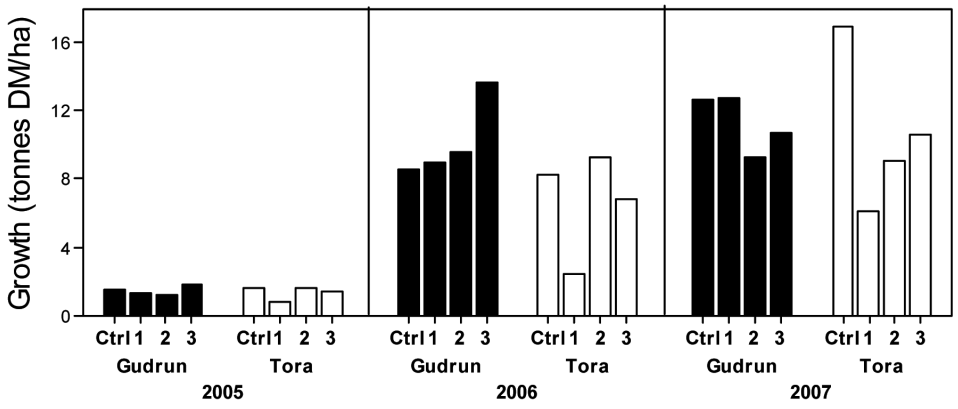


FIGURE 3
Annual shoot growth 2005–2007 (tonnes DM/ha).

A closer look at the inverted sections from the individual investigation lines revealed that the resistivity changed gradually during the experiment, as shown by the selected examples from line AA (Fig. 7). A decrease in resistivity developed underneath each irrigation pipe (Fig. 7a), where the zone of decreased resistivity initially had a vertical appearance. The depth of these zones increased over time to more than 2 m. The zones of decreased resistivity also spread laterally, creating a more diffuse layer with

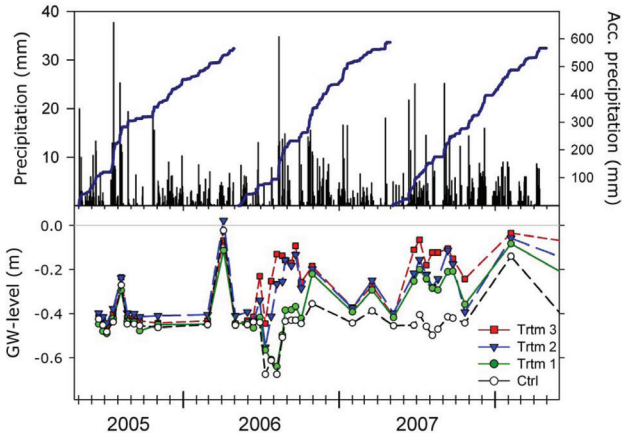


FIGURE 4
Daily and accumulated precipitation and groundwater level in the different treatments (mean of two observations).

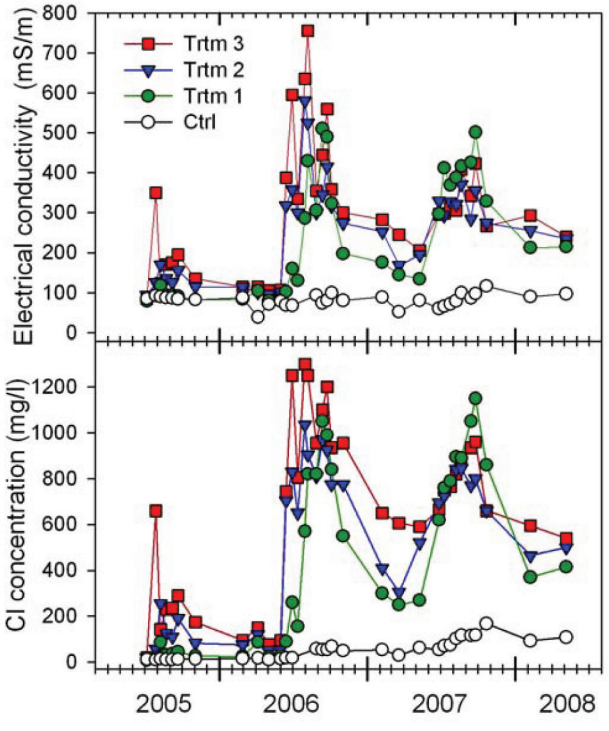


FIGURE 5
Electrical conductivity and concentration of chloride in superficial groundwater (mean of two observations).

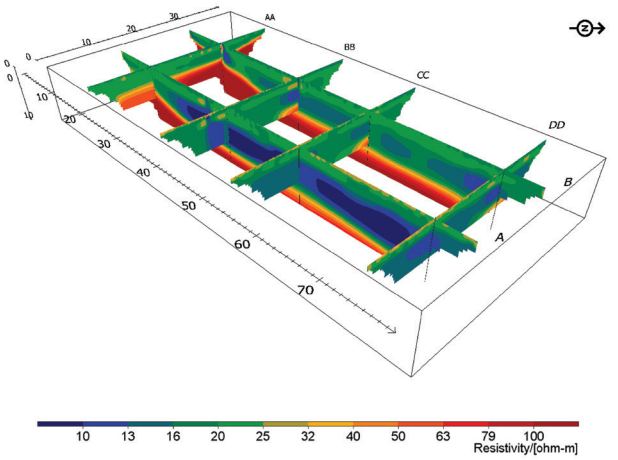


FIGURE 6
Overview of resistivity sections from 7–8 July 2005 (background resistivity survey). Lines A and B are 80 m long with direction SW-NE, while lines AA, BB, CC and DD are 40 m long with direction SE-NW. Maximum presented depth is 10 m for the longer lines and 5 m for the shorter lines.

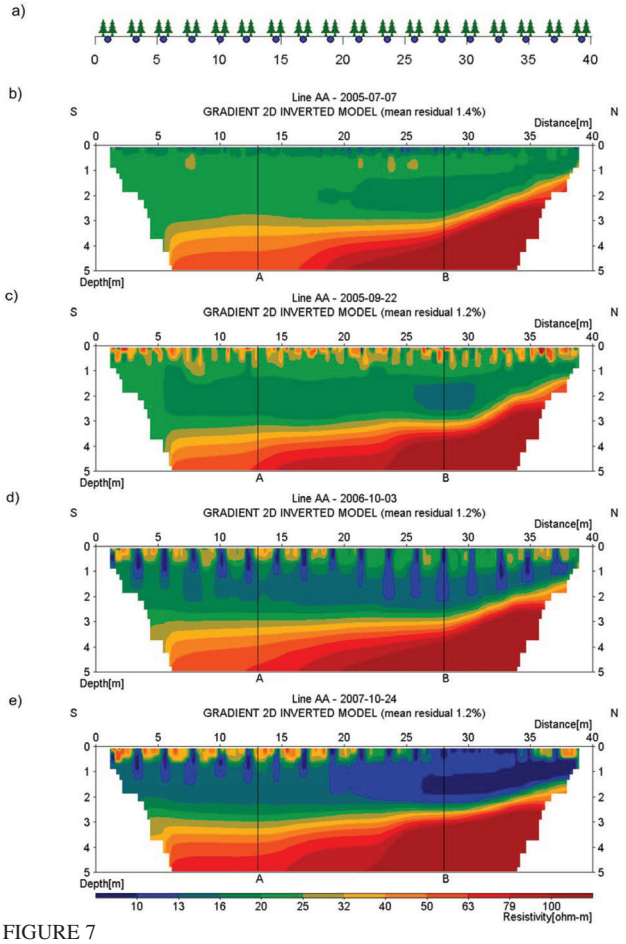


FIGURE 7
a) Location of irrigation pipes (●) and plant rows (▲). Examples of inverted resistivity sections from line AA (treatment 1): b) July 2005 before start of irrigation, c) September 2005, d) October 2006 and e) October 2007.

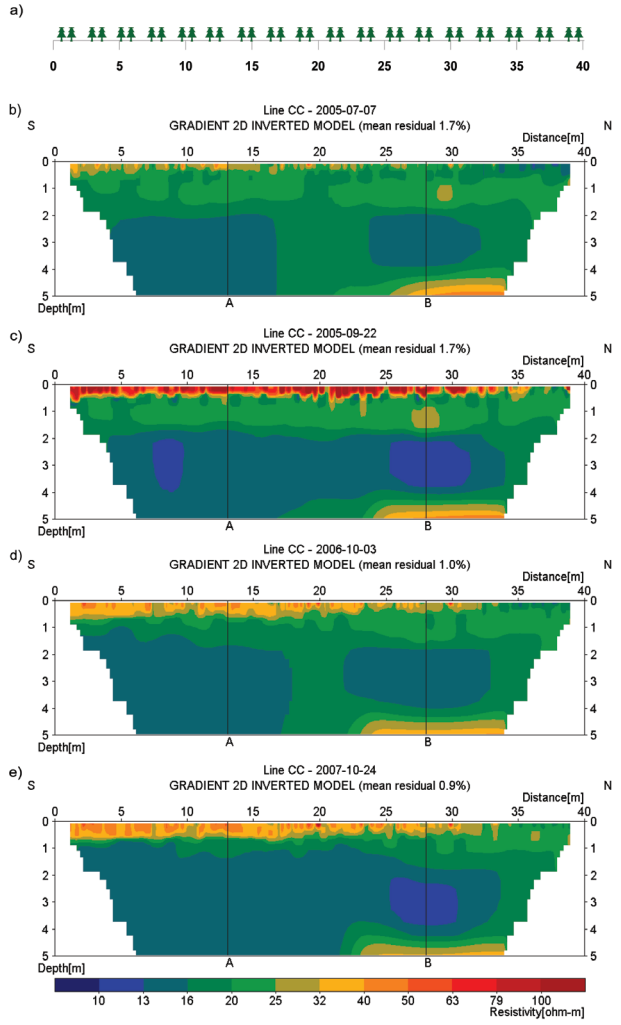


FIGURE 8

a) Location of plant rows (🌲). Examples of inverted resistivity sections from line CC (control = no leachate irrigation): b) July 2005, c) September 2005, d) October 2006 and e) October 2007.

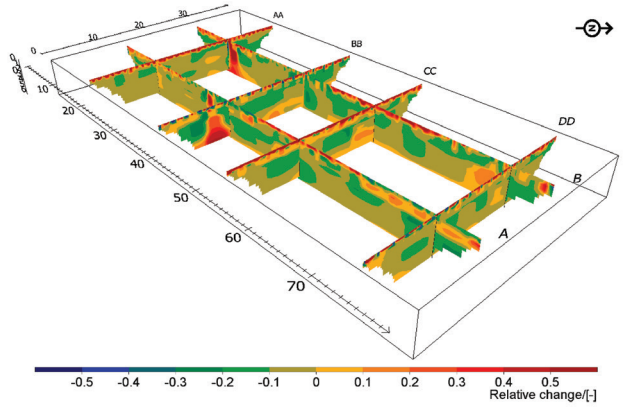


FIGURE 9

Overview of sections showing the relative change in resistivity from the background survey 7–8 July 2005 until 21–22 September 2005. The maximum presented depth in the sections is 6 m.

decreased resistivity. As a comparison, the corresponding inverted section from the control treatment (Fig. 8), the one with no leachate irrigation, shows that the zones of concentrated decrease in resistivity beneath the irrigation pipes are absent.

There was also a very distinct increase in resistivity (yellow-red colour) around each plant row, as shown in the detailed section from line AA (Fig. 7). The extent of these zones also increased over time. These changes started on a small scale close to the soil surface and gradually expanded in magnitude and size over time. In the line from the control treatment, line CC, the near-surface zones of increasing resistivity remain and are more prominent (Fig. 8), forming an almost continuous uppermost zone of higher resistivity.

Figures 9–11 show an overview of the change in resistivity, relative to the background resistivity measured at the start of the experiment, for three selected occasions at the end of each of the three growing seasons (21–22 September 2005, 3–4 October 2006 and 24–25 October 2007 relative to 7–8 July 2005). A

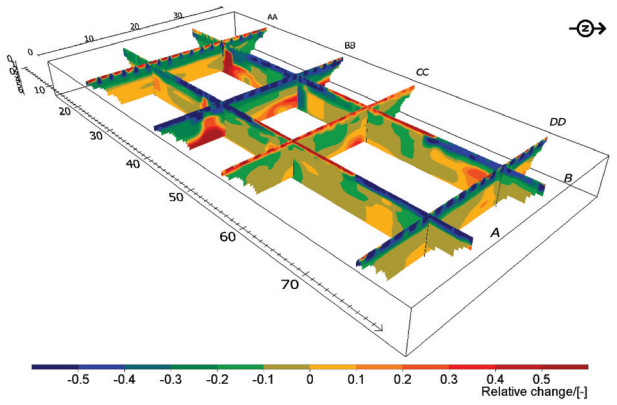


FIGURE 10

Overview of sections showing the relative change in resistivity from the background survey 7–8 July 2005 until 3–4 October 2006. The maximum presented depth in the sections is 6 m.

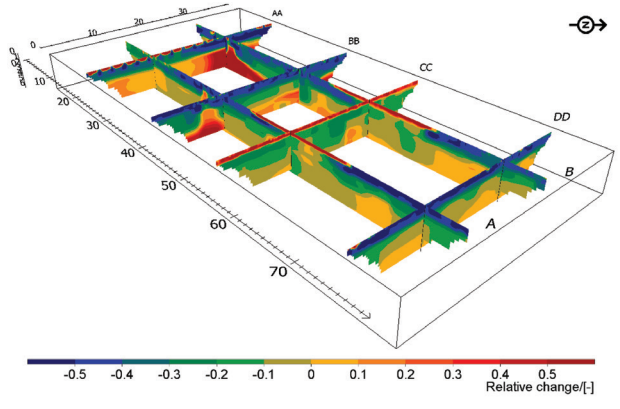


FIGURE 11

Overview of sections showing the relative change in resistivity from the background survey 7–8 July 2005 until 24–25 October 2007. The maximum presented depth in the sections is 6 m.

negative change (blue-green) indicates that the resistivity had decreased, whereas a positive change (yellow-red) indicates an increase in resistivity.

The different investigation lines (Figs 9–11) show the changes in resistivity over time in plots with different irrigation regimes. This is visible along lines A and B with the largest decrease in resistivity in the 20–40 m sections (treatment 3 – line BB) and 60–80 m sections (treatment 2 – line DD) during 2005 and 2006 (Figs 9 and 10). The zones of increasing resistivity in connection with the double plant rows are very distinct.

In Figs 10 and 11, it is also apparent that a lateral spread of low resistivity occurred. There are indications of a 'plume' of low resistivity spreading from treatment 3 (20–40 m) into the control treatment (40–60 m), as well as from treatment 2 but to a lesser extent (Fig. 10).

DISCUSSION

Groundwater level

The variation in the groundwater level between treatment 1 and the control could have been due to the much higher growth in the latter, since transpiration is highly correlated with growth (Lindroth and Båth 1999; Linderson *et al*. 2007).

Groundwater chloride concentration and electrical conductivity

The increase in Cl^- concentration in the control treatment (Fig. 4) may be an indicator of slight cross-contamination between plots through lateral transport in the saturated zone. This is in line with the observed 'plume' of decreased resistivity spreading laterally, mainly from treatment 3 into the control treatment (Figs 10 and 11).

Resistivity imaging

The spatial differences in resistivity in the lower layer (Fig. 6) may be due to differences in clay content, as the south-eastern part of the area is reported to have less clay.[1] Furthermore, the inverted model sections displayed high resistivity at the bottom for lines A, BB and AA. This could have been caused by shallow bedrock but may also be due to a layer of coarse-grained soil between the more clayey upper soil and the bedrock. However, auger drilling before insertion of the groundwater pipes at the line intersections reached a maximum depth of 1.8 m and did not penetrate to any such coarse-grained layer or rock. The decline in resistivity at a depth of about 1 m was probably caused by increased water content, as it more or less coincided with the groundwater level.

A decrease in resistivity can be expected if the soil water or salt content increases. It is likely that the size of the zone of increasing resistivity, for example line AA (Fig. 7), is closely related to the development of the plant root system. This leads to the assumption that the increase in resistivity is caused by water extraction by plant roots. In Fig. 7(d,e), it is apparent that the effect of the plants is less pronounced at a distance 20–40 m along line AA compared with a distance of 0–20 m. Distance 20–40 m corresponded to cv. Tora in treatment 1, which had roughly half the growth of cv. Gudrun (distance 0–20 m). We already noted differences in the groundwater level between these treatments, which were most likely explained by lower transpiration caused by the much lower growth of cv. Tora.

The decrease in resistivity around the irrigation pipes (e.g., Figs 7 and 8) is probably due mainly to an increased salt content resulting from landfill leachate irrigation. In the control treatment that received tap water in amounts similar to the amount of

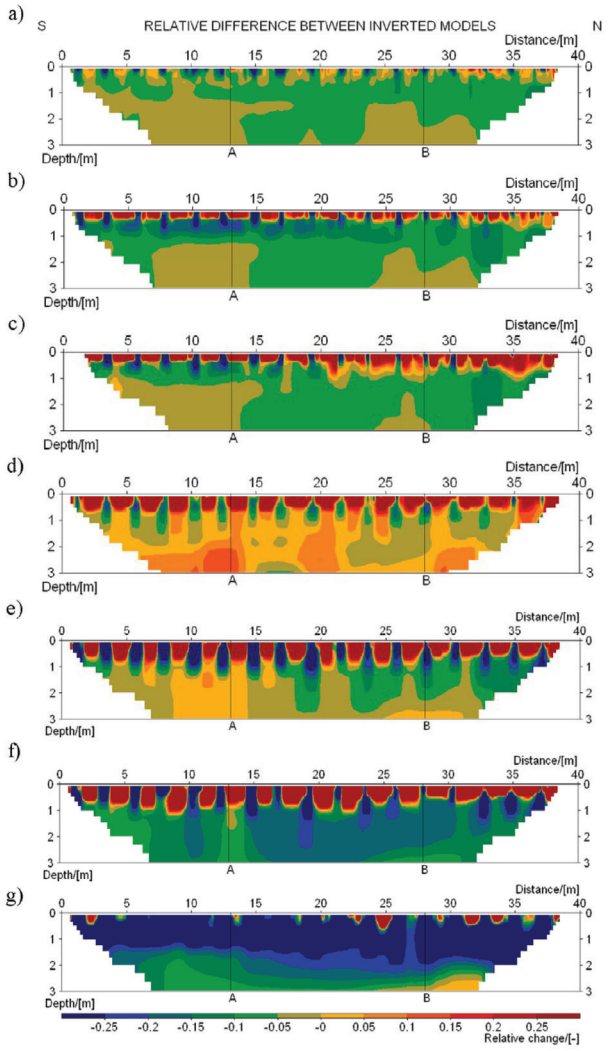


FIGURE 12
Model of resistivity sections for line DD, showing the relative change in resistivity relative to the background survey 7–8 July 2005; a) 2 August 2005, b) 24 August 2005, c) 21–22 September 2005, d) 29 May–1 June 2006, e) 23–25 June 2006, f) 24–26 July 2006 and g) 3–4 October 2006. The position of the lines A and B intersection is marked.

[1] Oral communication of results from soil sampling carried out by Ragn-Sells Avfallsbehandling AB.

landfill leachate applied in treatment 2, there was instead an increase in resistivity over time in the upper soil layer. This indicates the large impact on resistivity caused by the added salt, which apparently accumulated in the soil.

The lateral spread of zones of decreasing resistivity (e.g., Fig. 7) may be due to increasing amounts of high-conductivity irrigation water moving more or less vertically in the unsaturated zone and starting to spread laterally once it reaches the saturated zone. The most likely explanation for the lateral spread in decreased resistivity is that lateral transport of groundwater occurred between the plots, i.e., what appeared to be a plume was in fact slow diffusion or mass transport of high-ionic water in the groundwater zone between the plots. This is supported by the increase in Cl331 concentration in the samples taken in the control treatment (Fig. 4). However, judging from the small increase in groundwater Cl^- concentration over time in the control treatment, this diffusion/transport was relatively limited and did not significantly disturb the analyses of groundwater obtained from the different plots in the field. Thus, the method of sampling shallow groundwater for leaching estimates from separate, adjacent field plots, as described in our previous paper (Aronsson *et al*. 2010), seems to be relevant.

The zone of increased resistivity underneath each double row of plants can be attributed to soil drying and/or plant uptake of dissolved ions by the roots. The depth and lateral extent of these zones increased over time, which coincides with the expected development of the plant root systems. The increase was most pronounced for lines BB (treatment 3) and CC (control treatment). When comparing lines AA (treatment 1) and CC there was only a small difference after the first year (Fig. 9), indicating that the plants consumed more or less all water and ions applied to treatment 1 during the first year of the experiment. However, after the second (Fig. 10) and third (Fig. 11) years of the experiment, the differences between lines AA and CC were pronounced, especially in the deeper soil layers, indicating a substantial excess supply of water and/or ions through the leachate irrigation. As proposed by Rossi *et al*. (2011), the resistivity images could be used to guide sampling and other *in situ* investigations of roots and root-related processes.

If the zones of increased resistivity indeed corresponded to the root zone, this suggests that the roots had grown to a 1 m depth or more during 2006, as shown by the relative change in soil resistivity (Fig. 12f). Very intense rain during August 2006 saturated the ground in the latter part of the growing season, which to a large extent eliminated the differences in resistivity observed previously (Fig. 12g).

As shown in Fig. 12, there were also differences between cvs. Gudrun and Tora as regards root development and water use in treatment 2 (line DD) during 2005 (most obvious in e.g., Fig. 12c but also visible in Fig. 9). Drying (increased resistivity) appeared to be more pronounced for cv. Tora (20–40 m) during 2005. Furthermore, root depth appeared to be larger for cv. Tora than for cv. Gudrun (e.g., Fig. 12c and Fig. 9). In 2005, cv. Tora had a growth of 1.6 tonnes DM/ha, whereas cv. Gudrun had growth of 1.2 tonnes DM/ha, which might explain the differences in root development as indicated by differences in soil resistivity. However during 2006, the relative growth situation was reversed (Fig. 12d–f).

An area around the intersection of line AA and line B demonstrated very low resistivity throughout 2007 (Fig. 11). The extension at the surface expanded laterally over time, as illustrated by the example from line AA in October 2007 (Fig. 7e). This area coincided with an extensive die-back of the crop recorded in late 2008. Plant die-back would lead to a decrease in transpiration and hence wetter ground, which in turn would reduce the resistivity. The cause of the die-back is not known.

The anomalous zone of increased resistivity that is visible in the different sections close to the intersection of lines AA and A coincides with a copper rod that was inserted to around 1.0 m in the ground at this point before the first resistivity measurements were carried out and that was removed before the time of the first resistivity section (Fig. 9). The rod was used for grounding a TDR system. In previous resistivity sections there was a negative anomaly (not shown), probably caused by irrigation resulting in improved contact between the metal rod and the ground. When the metal rod was removed, a positive difference anomaly resulted from the removal of the conductive material.

Furthermore, there was a very significant increase in resistivity at depth around the intersection of lines AA and B that cannot be explained by any other observations. It might have been caused by inversion artefacts, for example the very strong contrast between the overlying strata might have caused overshooting in the inversion models. Another possibility is 3D effects, i.e., an influence from change in resistivity next to the line rather than below it.

One factor that may be significant for the temporal variation in resistivity apart from changes in water and ion content is temperature. A decrease in temperature increases the resistivity and vice versa, with a decrease from 20ºC to 0ºC resulting in an almost twofold increase in resistivity (e.g., Hayley *et al*. 2007). Although this effect was not considered in this study, it will have to be taken into account and corrected for in order to allow subtle effects to be interpreted and quantitative studies to be carried out (e.g., Hayley *et al*. 2010).

CONCLUSIONS

Models of resistivity distribution in soils can be very useful for the detection of variations in soil composition and in water and ion content but the results can be ambiguous since more than one of these factors may be the cause of higher or lower resistivity. Analysis of time series measurements of soil resistivity is a powerful tool for monitoring changes in water and ion content and can remove these ambiguities. By analysing the change in resistivity, the local variation in soil resistivity, for example due to variation in clay content, is removed and the results reflect temporal variation due to changes in water and ion content. This allows evaluation of more subtle variations in soil properties and

of the effect of processes. Changes in resistivity observed in this study were clearly linked to differences in irrigation quantities and plant growth. The results show that resistivity monitoring in 2D and 3D has strong potential for irrigation applications.

Soil resistivity measurements can be used not only to monitor transport of water and solutes in the soil but also to indirectly study the development of plant root systems via the magnitude of soil volume affected by the presence of plant roots, assuming that the degree of water saturation or ion content is affected by the roots. If applied with higher resolution, i.e., with shorter distances between the electrodes and within the grid, it is likely that non-destructive 3D images of the growth of root systems could be produced. The resistivity results clearly confirmed that the groundwater sampling method applied in this study is a relevant and fairly accurate method for groundwater monitoring.

ACKNOWLEDGEMENTS

The resistivity field data acquisition was carried out by Ragn-Sells Avfallsbehandling AB, who also funded data processing and analyses plus investigations with other methods. ABEM Instrument AB provided the resistivity instrumentation and trained the staff at Ragn-Sells Avfallsbehandling AB in its use.

REFERENCES

Aronsson P., Dahlin T. and Dimitriou I. 2010. Treatment of landfill leachate by irrigation of willow coppice – Plant response and treatment efficiency. *Environmental Pollution* **158**, 795–804.

Auken E., Pellerin L., Christensen N.B. and Sørensen K. 2006. A survey of current trends in near-surface electrical and electromagnetic methods. *Geophysics* **71**(5), G249–437, G260.

Besson A., Cousin I., Bourennane H., Nicoullaud B., Pasquier C., Richard G. *et al*. 2010. The spatial and temporal organization of soil water at the field scale as described by electrical resistivity measurements. *European Journal of Soil Science* **61**, 120–132

Binley A., Henry-Poulter S. and Shaw B. 1996. Examination of solute transport in an undisturbed soil column using electrical resistance tomography. *Water Resources Research* **32**, 763–769.

Dahlin T. 2001. The development of DC resistivity imaging techniques. *Computers and Geosciences* **27**, 1019–1029.

Dahlin T. and Zhou B. 2006. Multiple-gradient array measurements for multichannel 2D resistivity imaging. *Near Surface Geophysics* **4**, 113–123.

Dimitriou I. and Aronsson P. 2007. Landfill leachate treatment on short-rotation willow coppice: Resource instead of waste? In: *Landfill Research Focus,* (ed. Ernest C. Lehmann), pp. 55–85. Nova Science Publishers, Inc. ISBN 1-60021-775-3.

French H. and Binley A. 2004. Snowmelt infiltration: Monitoring temporal and spatial variability using time-lapse electrical resistivity. *Journal of Hydrology* **297**(1), 174–186.

Gebbers R., Lück E., Dabas M. and Domsch H. 2009. Comparison of instruments for geoelectrical soil mapping at the field scale. *Near Surface Geophysics* **7**(3), 179–190.

Guerin R., Munoz M.L., Aran C., Laperrelle C., Hidra M., Drouart E. and Grellier S. 2004. Leachate recirculation: Moisture content assessment by means of a geophysical technique. *Waste Management* **24**, 785–794.

al Hagrey S.A., Schubert-Klempnauer T., Wachsmuth D., Michaelsen J. and Meissner R. 1999. Preferential flow: First results of a full-scale flow model. *Geophysical Journal International* **138**(3), 643–654.

Hayley K., Bentley L.R., Gharibi M. and Nightingale M. 2007. Low temperature dependence of electrical resistivity: Implications for near surface geophysical monitoring. *Geophysical Research Letters* **34**, L18402.

Hayley K., Bentley L.R. and Pidlisecky A. 2010. Compensating for temperature variations in time-lapse electrical resistivity difference imaging. *Geophysics* **75**(4), 467, WA51–WA59.

Jones G.M., Cassidy N.J., Thomas P.A., Plante S. and Pringle J.K. 2009. Imaging and monitoring tree-induced subsidence using electrical resistivity imaging. *Near Surface Geophysics* **7**(3), 191–206.

Kemna A., Kulessa B. and Vereecken H. 2002. Imaging and characterisation of subsurface solute transport using electrical resistivity tomography (ERT) and equivalent transport models. *Journal of Hydrology* **267**, 125146.

Leroux V. and Dahlin T. 2005. Time-lapse resistivity investigations for imaging saltwater infiltration in glaciofluvial deposits. *Environmental Geology* **49**(3), 347–358.

Linderson M.-L., Iritz Z. and Lindroth A. 2007. The effect of water availability on stand-level productivity, transpiration, water use efficiency and radiation use efficiency of field-grown willow clones. *Biomass and Bioenergy* **31**, 460–468.

Lindroth A. and Båth A. 1999. Assessment of regional willow coppice yield in Sweden on basis of water availability. *Forest Ecology and Management* **121**, 57–65.

Loke M.H., Acworth I. and Dahlin T. 2003. A comparison of smooth and blocky inversion methods in 2-D electrical imaging surveys. *Exploration Geophysics* **34**(3), 182–187.

Öman C., Malmberg M. and Wolf-Watz C. 2000. Handbok för Lakvattenbedömning – Metodik för karakterisering av lakvatten från avfallsupplag (in Swedish.). IVL rapport/report B 1354. IVL Svenska Miljöinstitutet AB. http://www3.ivl.se/rapporter/pdf/B1354.pdf

Palacky G.J. 1987. Resistivity characteristics of geologic targets. In: *Electromagnetic Methods in Applied Geophysics,* (ed. M.N. Nabighian), pp. 53–130. Society of Exploration Geophysics.

Rosqvist H., Dahlin T. and Lindhé C. 2005. Investigation of water flow in a bioreactor landfill using geoelectrical imaging techniques. *Proceedings of Sardinia-05, 10th International Waste Management and Landfill Symposium*, Cagliari, Sardinia, Italy.

Rossi R., Amato M., Bitella G., Bochicchio R., Ferreira Gomes J.J., Lovelli S. *et al*. 2011. Electrical resistivity tomography as a non-destructive method for mapping root biomass in an orchard. *European Journal of Soil Science* **62**(2), 206–215.

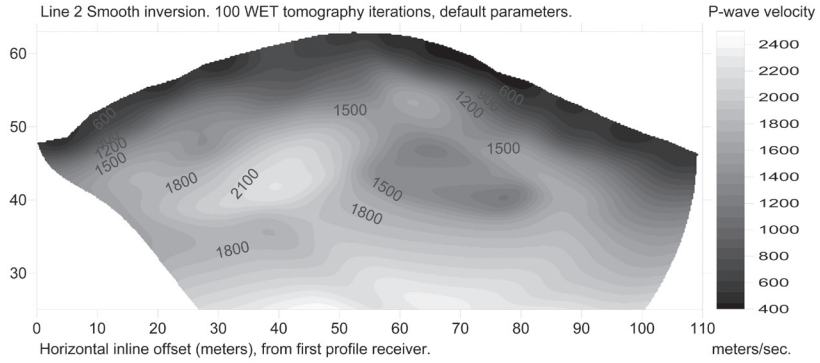
Samouëlian A., Richard G., Cousin I., Guérin R., Bruand A. and Tabbagh A. 2004. Three-dimensional crack monitoring by electrical resistivity measurement. *European Journal of Soil Science* **55**(4), 751–762.

Seladj S., Cosenza P., Tabbagh A., Ranger J. and Richard G. 2010. The effect of compaction on soil electrical resistivity: A laboratory investigation. *European Journal of Soil Science* **61**(6), 1043–1055.

Sjödahl P., Dahlin T., Johansson S. and Loke M.H. 2008. Resistivity monitoring for leakage and internal erosion detection at Hällby embankment dam. *Journal of Applied Geophysics* **65**, 155–164.

Slater L.D. and Sandberg S.K. 2000. Resistivity and induced polarization monitoring of salt transport under natural hydraulic gradients. *Geophysics* **65**, 408–420.

INTELLIGENT RESOURCES INC. offers **RAYFRACT®** Seismic Refraction & Borehole Tomography software : velocity structure imaging for engineering and exploration



Intelligent Resources Inc.
142-757 West Hastings Street
Vancouver BC V6C 1A1
Canada

Phone +1 604 782-9845
Web http://rayfract.com
E-mail rayfract@gmail.com

350 full licenses sold.

Our Rayfract® traveltime tomography software models refraction, transmission and diffraction of seismic waves, with Fresnel volumes. Import or pick first breaks then run our Smooth inversion or DeltatV+XTV methods. Supports extreme topography, strong lateral velocity variation, local velocity inversions. Uses multiple CPU cores. Invert crosshole and downhole VSP surveys. Build synthetic models with Surfer®, forward model traveltimes. Plot Plus-Minus, Wavefront, CMP refractors on tomogram. Import SEGY and SEG-2 trace files, compatible with most seismographs. Flexible trace display, frequency filtering, shot stacking. Reads third-party ASCII file formats with first breaks and recording geometry. Standard license price is US $ 2,200.00 including one year of support. Price reduction of 20% for academic and non-profit use. Visit our web site for latest release notes, updated help file, free trial, tutorials and published benchmark comparisons. Rent our software. Resellers welcome.

Copyright © 1996-2014 Intelligent Resources Inc. RAYFRACT is a registered trademark of Intelligent Resources Inc. Canadian Business No. 86680 1236. British Columbia PST No. PST-1015-0246. Requires Golden Software's Surfer for plotting.

EAGE
EUROPEAN ASSOCIATION OF GEOSCIENTISTS & ENGINEERS

Saint Petersburg 2014

Geosciences – Investing in the Future

Register now!

6th Saint Petersburg International Conference & Exhibition

7-10 April 2014
Saint Petersburg, Russia

www.eage.org
www.eage.ru